Time-resolved far-infrared magnetospectroscopy of hydrogenlike impurities in III-V semiconductors

G. L. J. A. Rikken* and P. Wyder

Max-Planck-Institut für Festkorperforschung, Boîte Postale 166X, F38042, Grenoble Cédex, France

J. M. Chamberlain and G. A. Toombs

Physics Department, Nottingham University, Nottingham NG7 2RD, United Kingdom

L. L. Taylor

Royal Signals and Radar Establishment, Great Malvern, Worcestershire WR14 3PS, United Kingdom

Time-resolved far-infrared magnetospectroscopic studies of the photoconductive response of very-high-purity ($\mu \gtrsim 10^5$ cm^2 V^{-1} s^{-1}) n-type InP are reported from 2 to 20 K using a pulse-slice laser. The decay of the photoconductive response is studied for a variety of sample temperatures and compensation ratios for resonant $1s$-$2p_+$ and cyclotron resonance conditions. Decay schemes are proposed to account for the observed behavior of the lifetimes as a function of magnetic field. A calculation of the transition rates for acoustic-phonon-assisted decay in a magnetic field is presented for the decay channels proposed.

I. INTRODUCTION

In the last two decades far-infrared (FIR) magnetospectroscopy has been used to probe in detail the shallow donor[1] impurity levels, and to a lesser extent, the shallow acceptor levels of III-V semiconductors.[2] Such investigations have used cw spectroscopic techniques to reveal that, to a high degree, the shallow impurity state is analogous to the hydrogen atom. Transitions involving both the ground and excited states, and among excited states only,[3] have been examined. Analogues of the free-space H$^-$ ion[4] and the H$_2$ molecule[5] have been observed, and a sensitive assay technique for inadvertent shallow contaminants at the 10^{-14}-cm^{-3} level has been developed.[6] In parallel with this considerable experimental effort, theoretical studies of neutral hydrogenlike systems have abounded,[7] with especial reference to the determination of energy levels in a magnetic field using appropriate numerical or variational techniques. The magnetic quantisation of the energy levels of free electrons into Landau levels (LL) has led to speculation on the possibility of constructing a tuneable solid state FIR laser source. All the descriptions of these effects require a knowledge of the lifetimes of electrons in both bound and free states and the transition rates between these states: Such information cannot easily be obtained from cw magnetospectroscopy.

The use of time-resolved (TR) FIR methods to investigate the relaxation processes for electrons photoexcited from shallow impurities is, however, a comparatively novel field. Clearly TR spectroscopy offers advantages over indirect techniques, such as saturation-absorption spectroscopy[8] (which relies for interpretation on predicated recombination models), or over other direct probes of electron recombination dynamics such as electrical excitation[9] or pulsed optical excitation at shorter wavelengths.[10] The TR FIR spectroscopic technique reported here enables the dynamics of individual transitions to be monitored by appropriate choice of laser frequencies and tuning of the magnetic field. In addition, the experimental conditions can be chosen to ensure that the electron population is in quasiequilibrium with the lattice; this condition cannot always be assured in an electrical pulse or short-wavelength laser measurement. The importance of the realization of this condition has been discussed elsewhere.[10]

The most sensitive experimental technique for cw magnetospectroscopy involves the measurement of the photoconductive (PC) response of the sample to FIR radiation. The mechanism generally accepted for this process[11] is that following photoexcitation electrons return to the ground state via intermediate bound states with the emission of acoustic phonons. The deexcitation process has been analyzed in detail by many workers.[12] Transition rates obtained from this analysis indicate that the rate determining step in the decay process is a bottleneck at the $2s$ state in zero magnetic field. In the presence of a magnetic field, saturation-absorption experiments in GaAs (Ref. 8) and direct TR studies[13] in InP indicate that the $2p_-$ state is also likely to act as a bottleneck in the decay process.

Although several calculations of the optical transition rates in magnetic fields have been given in the literature,[12,14] there appears to be a conspicuous absence of calculations of rates for *phonon*-assisted transitions which are believed to be dominant.

It is the purpose of the present paper to report an experimental study of TR FIR magnetospectroscopy using PC detection in a number of samples of high-purity InP grown by metal oxide chemical vapor deposition

(MOCVD) and chloride vapor-phase epitaxy (VPE). The samples have differing degrees of compensation, and one aim of the work is to investigate the effect that this may have on lifetimes in view of the evidence of indirect measurements in GaAs.[8,15] The PC is investigated in magnetic fields up to 8 T, and the decay of the photosignal for both the resonant $1s$-$2p_+$ and cyclotron resonance (CR) PC is monitored. FIR pulses of duration 10–50 ns and rapid cutoff time ($\lesssim 1$ ns) are used to excite the PC in the samples. The use of this fast-pulse technique enables effects indicated in previous longer-pulse studies[13] to be systematically explored. Decay schemes are proposed to account for the observed behavior of the lifetimes as a function of magnetic field. A calculation of the transition rates for acoustic-phonon-assisted decay in a magnetic field is presented for the decay channels proposed. To the knowledge of the present authors this is the first time that such a calculation has been given in the literature. The behavior of energy-relaxation lifetimes in n-type GaAs for processes involving Landau level (LL) and impurity levels (IL) has been deduced from saturation-absorption measurements.[8,15] Other techniques used to measure or infer such lifetimes include cyclotron resonance induced conductivity[16] and FIR cyclotron emission under hot-electron conditions.[17] Allan et al.[8] state that the rate determining step for the effective lifetime of a conduction band electron in the bottom ($N=0$) LL, hereafter referred to as τ_{eff}, is the transfer of such electrons from the $2p_+$ to the $N=0$ LL. τ_{eff} is found by these workers to be independent of N_a and to decrease in a magnetic field. Müller et al.[18] have studied the saturation absorption, cyclotron emission and PC decay following excitation by a voltage pulse or a long-wavelength laser pulse for InSb. They conclude that the lifetime of the $2p_+$ state is independent of N_a and decreases with magnetic field. Bluyssen et al.[16] deduce that τ_{eff} is of the order 1–100 ns, decreasing smoothly with increasing temperature. This conclusion is strengthened by a direct measurement of PC decay in GaAs. Allan et al.[8] have studied the electron concentration dependence of the $N=1$ LL lifetime and noted that for electron density greater than 10^{12} cm^{-3} this quantity falls with electron density due to electron-electron scattering.

In Sec. II we discuss the experimental arrangement and sample characteristics used in our measurements. In Sec. III the energy level diagram used to interpret the data is briefly reviewed. In Sec. IV the theory of phonon-assisted transition rates in a magnetic field is given, but the details are confined to the Appendix. Finally, in Sec. V the experimental results are presented as a function of both temperature and magnetic field. These results are also discussed in that section.

II. EXPERIMENT

Samples of high-purity epitaxial indium phosphide were used in this investigation:[19] The electrical properties of these samples are listed in Table I. The specimens were provided with Ohmic contacts and mounted in an 8-T cryostat with light pipe access. Pulses of FIR radiation with controllable width (10–50 ns) and sharp cutoff

TABLE I. Electrical properties of the samples used. μ, N_d, and N_a are, respectively, the mobility and donor and acceptor concentrations.

Sample	μ (77 K) (cm^2 V^{-1} s^{-1})	$N_d - N_a$ (77 K) (10^{14} cm^{-3})	N_a / N_d
1	123 000	1.2	0.61
2	133 000	3.7	0.05
3	76 000	3.7	0.62

(~ 1 ns) were generated by a pulse-slice laser system. The pulse slicing arrangement is described fully elsewhere.[20] The maximum laser power at the sample was 100 W cm^{-2}: This intensity was attenuated when necessary.

In view of the possibility of impact ionization phenomena and the formation of "tails" in the photoresponse of InP even for modest sample bias voltages,[13] the bias applied to the samples is kept low (< 1 V cm^{-1}). The experiments were performed in the constant voltage mode. The signal generated across a 50-Ω resistor in series with the sample was initially amplified by wide-band (0.6 GHz) amplifiers. Data acquisition for the investigation of the time-integrated spectral response as a function of magnetic field was accomplished with a conventional boxcar system. A Tektronix transient analyzer was used to monitor the decay of the PC after cessation of the laser pulse for TR measurements. On occasions up to 2000 pulses were averaged to obtain typical experimental results as shown in Fig. 1.

At high exciting FIR intensities, Auger and impact reexcitation effects can be important, even at very-low-bias electric fields,[21,22] and the decay curve cannot be described by a single parameter. However at low intensity ($n \ll N_a$) one can analyze data of the type shown in Fig. 1 with a simple analytical expression of the form
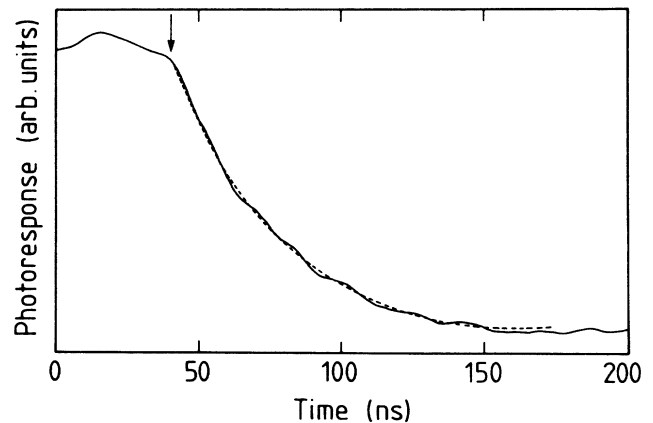

FIG. 1. Decay of the resonant $1s$-$2p_+$ photosignal after termination of a $\lambda = 148.5$-μm-wavelength pulse for sample 2 at 4.2 K under low-bias conditions. The magnetic field is 5.90 T. The dashed line is an exponential fit to the data.

$$n(t) = n_0 \exp(-t/\tau_{eff}) , \qquad (2.1)$$

thus obtaining a value for the effective lifetime τ_{eff}.

III. RECOMBINATION MODELS

Although the present experimental techniques provide a direct measurement of τ_{eff} it is necessary first to present a brief outline of the recombination models used to interpret the measured variation of this quantity with magnetic field and temperature for the cases of resonant $1s$-$2p_+$ and CR photoconductivity.

First the $1s$-$2p_+$ case will be considered. From the well-known diagram of the energies of LL's and IL's in magnetic fields,[23] confirmed by copious previous experimental work, it can be concluded that at magnetic fields greater than approximately 3 T the $2p_+$ state is at a higher energy than the $N=0$ LL. This situation is depicted in Fig. 2(a). A FIR photon resonantly excites electrons from the $1s$ state, and under the present experimental conditions this photoionization process occurs very rapidly.[24] It is assumed that in the specimens used in this investigation conduction occurs in extended states only; for the case of Fig. 2 conduction in the $N=0$ LL is considered solely. With reference to Fig. 2(a), it may be seen that at the termination of the laser-pulse electrons will continue to enter the $N=0$ LL from the $2p_+$ state (accompanied by phonon emission) or from lower bound states (accompanied by phonon absorption). At fields less than about 3 T the $N=0$ LL will be populated by phonon absorption processes from the $2p_+$ level. For both magnetic field regimes the deexcitation is a cascade mechanism involving acoustic-phonon emission,[12] as illustrated.

Figure 2(b) illustrates the situation under CR conditions. The mechanism which gives rise to PC under CR conditions has been shown to be[16] the change in the $N=0$ population at resonance, rather than a significant change in electron mobility. The relative efficiencies of radiative and nonradiative transitions have been discussed elsewhere.[12] Under conditions of high magnetic field ($\gtrsim 10$ T

for InP) the $1s$ level will pin to the $N=0$ LL and the $2p_+$ level will pin to the $N=1$ LL.[25] It is evident that under such conditions the transitions depicted by the two figures become essentially identical.

Samples with a wide range of acceptor concentrations, N_a, are used in this work. Clearly the different numbers of ionized donors in these specimens may have an effect on the rate-determining steps in the deexcitation mechanisms illustrated in Figs. 2(a) and 2(b); This matter is considered further in Sec. IV.

Under conditions of relatively high excitation (number of excited carriers greater than 10^{13} cm^{-3}) it has been shown[18] that electron-electron interaction in the $N=1$ LL will scatter electrons to the $N=2$ LL, followed by fast (10^{-12} s) optical-phonon emission. The decrease of the $N=1$ LL lifetime when the electron concentration exceeds 10^{12}–10^{13} cm^{-3} has also been noted by Allan et al.[8] In the present experiments the laser intensity is sufficient to produce approximately 10^{13} cm^{-3} carriers and therefore electron-electron scattering effects cannot be ruled out.

In the present experiments, an effective lifetime, τ_{eff}, is measured under conditions of laser intensity and sample bias which always produce simple exponential decays of the photocurrent. The effects of laser intensity and sample bias have been considered elsewhere:[21,22] The present work primarily seeks to investigate magnetic field and temperature effects. The interpretation which we give to our measured quantity τ_{eff} (with order of tens of ns) is of an effective lifetime in the $N=0$ LL under conditions of carrier density equal to 10^{13} cm^{-3} and bias sufficiently low to prevent hot-electron effects. Deexcitation from higher LL's will occur on a much shorter timescale than this: It is argued (Sec. IV) that the determining factor for τ_{eff} is the rate for capture into bound states. This interpretation is at variance with that of other workers.[8]

IV. CALCULATION OF PHONON TRANSITION RATES IN A MAGNETIC FIELD

The rates for electronic transitions into and between hydrogenlike bound impurity states, accompanied by the absorption and emission of phonons, have been previously calculated in zero magnetic field.[14,26] The rates have been shown to be greater than those for optical transitions. Optical transition rates have also been calculated in a magnetic field.[27] In this section we investigate the effect of a magnetic field on a (phonon assisted) transition rate and use the results to interpret the PC decay times shown in Fig. 4.

In order to calculate these rates it is first necessary to know the wave functions and energy levels of the hydrogenlike impurity in the presence of a magnetic field. These are not known analytically and a variety of approaches have been used to determine them. The exact wave functions can be expanded into a set of functions and the resulting coupled differential equations for the multiplying functions solved,[28] or alternatively perturbation theory may be used.[29] However, the majority of authors have used some form of variational calculation. Yafet, Keyes, and Adams[30] (YKA), Wallis and Bowl-
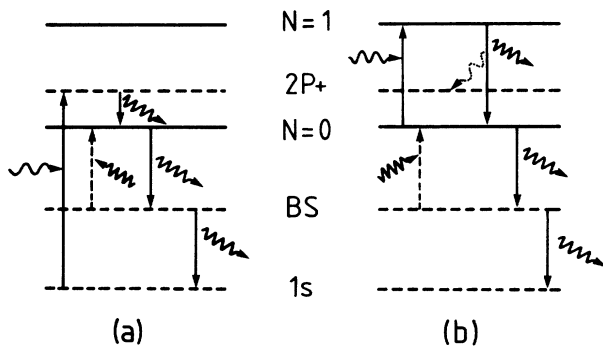

FIG. 2. Schematic of transitions between LL's (———) and IL's (— — —) for (a) $1s$-$2p_+$ resonant PC and (b) cyclotron resonance. BS represents a generalized bound state. Absorption of photons (wavy line) and absorption and emission of phonons (compressed wavy line) are represented in the conventional way. The dotted wavy line represents weak photon emission.

den,[31] and Narita and Miyao[32] have used a Gaussian type of trial wave function. This choice of wave function permits a considerable development of the problem and is accurate for very high fields when the magnetic potential is more important than the Coulomb potential. Other authors have used more hydrogenlike trial wave functions[33,34] or have used a large number of basis functions.[7] These latter treatments are numerical and do not have the simplicity of the Gaussian choice of trial wave function. Most of the calculations concentrate on the behavior of the energy levels in a magnetic field and give little information on the field-dependence of the wave functions. This is unfortunate since the behavior of the wave functions is just as important as that of the energy levels in determining the electronic transition rates.

In view of the lack of previous calculations of the phonon-assisted transition rates, we have performed the simplest possible calculation which reveals the physical features of the problem. Namely, we have calculated the transition rates using the YKA Gaussian choice of variational wave functions for the bound states and free-electron Landau-like wave functions for the continuum states. This choice allows analytic progress to be made, but the results can only be qualitative since the wave functions are always less accurately known than the energy levels in a variational calculation. The derivation of the transition rates is given in the Appendix, but the analysis is introduced here, together with a discussion of the results.

We have calculated the electronic transition rates in the presence of a magnetic field $\mathbf{B}$ in the z direction for transitions from the $2p_+$ state to the $N=0$ LL (Γ_C) and for the $N=0$ LL into a variety of bound states (Γ_B). We use λ to denote the set of quantum numbers for any state. The electronic transition rate $R_\lambda^{\lambda',\mathbf{q}}$ for an electronic transition from a state λ to a state λ' with emission of phonons of wave vector $\mathbf{q}$ is

$$f_\lambda(1-f_{\lambda'})(n_q+1)W_\lambda^{\lambda',\mathbf{q}} , \tag{4.1}$$

where n_q is the phonon occupation number for a state with phonons of wave vector $\mathbf{q}$ and frequency ω_q, and f_λ is the electron occupation number for state λ of energy E_λ. n_q will be given by a Bose-Einstein distribution for the phonons at the low temperature T, but f_λ is not an equilibrium electron distribution. f_λ will be determined by the dynamics of the photoconductive excitations and decays. $W_{\lambda'}^{\lambda,\mathbf{q}}$ is given from perturbation theory, using the Fermi golden rule, as

$$W_{\lambda'}^{\lambda,\mathbf{q}} = \frac{2\pi}{\hbar}\langle\lambda|\hat{H}_\mathbf{q}|\lambda'\rangle^2\delta(E_{\lambda'}-E_\lambda-\hbar\omega_q) , \tag{4.2}$$

where $\hat{H}_\mathbf{q}$ is the electron-phonon coupling for phonons of wave vector $\mathbf{q}$ as defined in Eq. (A1).

The transition rate $R_{\lambda',\mathbf{q}}^\lambda$ for a transition from state λ' to a state λ with absorption of a phonon is

$$f_{\lambda'}(1-f_\lambda)n_q W_{\lambda',\mathbf{q}}^\lambda \tag{4.3}$$

and $W_{\lambda',\mathbf{q}}^\lambda = W_\lambda^{\lambda',\mathbf{q}}$. The net transition rate into the state λ from λ' is

$$R_\lambda^{\lambda',\mathbf{q}} - R_{\lambda',\mathbf{q}}^\lambda = [f_\lambda(1-f_{\lambda'})+(f_\lambda-f_{\lambda'})n_q]W_\lambda^{\lambda',\mathbf{q}} . \tag{4.4}$$

The second factor can be neglected for $\hbar\omega_q \gg kT$ but this phonon absorption is important for transitions between states of similar energy. In the Appendix we outline the calculation of $W_\lambda^{\lambda',\mathbf{q}}$ for a variety of possible transitions.

We now draw attention here to some of the features of the results which are of importance in explaining the experimental data. All of the transition rates which we have calculated have a factor of the form

$$q_0^n \exp(-2a^2 q_0^2) , \tag{4.5}$$

where n is typically 2, $q_0 = \Delta E_B/\hbar v_s$, v_s is the sound velocity in InP and ΔE_B is the energy separation of the two levels and

$$a^2 = a_\lambda^2/(1+a_\lambda^2/l_B^2)^2 , \tag{4.6}$$

In (4.6) a_λ is the length scale for the cylindrical orbit of the bound state as defined in Eq. (A2) and $l_B = (\hbar/eB)^{1/2}$ is the magnetic length. The wave vector q_0 is defined [see below (A10)] for $k_z = 0$. The factor (4.5) which occurs in (A11) and (A12) accounts for the dropoff of the decay times for large magnetic fields B. The other factors in the transition rate also depend on B, but it is the exponential dependence which dominates the behavior. In zero magnetic field, $a = a_\lambda \simeq 3.0\times10^{-8}$ m, typically, and $q_0 = 1.9\times10^8$ m^{-1} for $\Delta E_B = 0.6$ meV. At a field of 10 T, a_λ will have decreased considerably [typically by $\frac{2}{3}$ according to YKA (Ref. 30)], and $l_B = 8\times10^{-9}$ m. Therefore $2(aq_0)^2$ is reduced from 4.7 to 0.5 as B increases from zero to 10 T, on the assumption that ΔE_B remains unchanged. For many bound states, the energy levels run parallel to the $N=0$ LL over a wide range of B, so that this assumption is a good one. Thus the transition rate will increase by a factor of approximately 70-fold due to the exponential factor alone. The other factors will reduce this to some extent, so that the observed order-of-magnitude change in τ_{eff} over this field range is reasonable. Therefore the decrease of the PC decay time in field is seen to be a direct consequence of the shrinkage of the bound state perpendicular to B. This shrinking of a_λ increases the matrix element, since there are less phonon wavelengths within its spatial extent.

Expression (4.5) has a maximum when $2(aq_0)^2 = 1$ for $n=2$. Therefore the transition rates are fastest for levels close to the $N=0$ level. However, if they are too close there will be a large probability of reexcitation to the conduction-band state due to phonon absorption. Therefore the optimum level for efficient removal of electrons probably lies 0.5–1 meV below the $N=0$ state: The $2s$ or the lower-lying $n=3$ states are likely candidates.

We next discuss the reason why the transition rate Γ_C is much faster than the rate Γ_B. Γ_C is the rate for transition from the $2p_+$ state into all the $N=0$ LL's by emission or absorption of a phonon. It follows from the sum over m in (A10) that the coupling is efficient for states with angular momentum $-|m|$, for which the expression

$$\frac{1}{|m|!}(c_\lambda a_\lambda q)^{2|m|} = \frac{1}{|m|!}\frac{a_\lambda^2 l_B q^{2|m|}}{a_\lambda^2+l_B^2} \tag{4.7}$$

is of order unity, since the terms in the summation decrease rapidly with increasing m. This implies electrons can scatter into states with m down to $-|m|$ $= -M \approx -4$ for typical values of parameters. The transition rate from all $N = 0$ levels (Γ_B': see Appendix) into a bound state is comparable with Γ_C. However, the PC decay rate involves transitions from particular $N = 0$ states into bound states of all impurities within range. If we average these over the range of k_z wave vectors, k_m, which are occupied by the electrons participating in the PC process, then

$$\Gamma_B \simeq \pi \Gamma_C / (1 + M) k_m d \ , \qquad (4.8)$$

where d is the impurity spacing and $M = 4$. Since $d < 10^{-7}$ m and $k_m = 5 \times 10^{-7}$ m^{-1}, then $\Gamma_B \simeq \Gamma_C / 8$. Thus the transition rate from the $2p_+$ into the $N = 0$ state is faster due to the difference in the number of available final states. From the results of the Appendix we estimate that $\Gamma_C \simeq 10^8 - 10^9$ s^{-1} for typical values of the parameters and therefore Γ_B is comparable with the observed PC times of several tens of nanoseconds.

V. RESULTS AND DISCUSSION

A. Temperature variation of effective lifetimes

Figure 3 shows the photoconductive decay time measured as a function of temperature for the low compensation sample (sample 2), for both CR and resonant $1s$-$2p_+$ PC. The sample bias is low in this case in order to
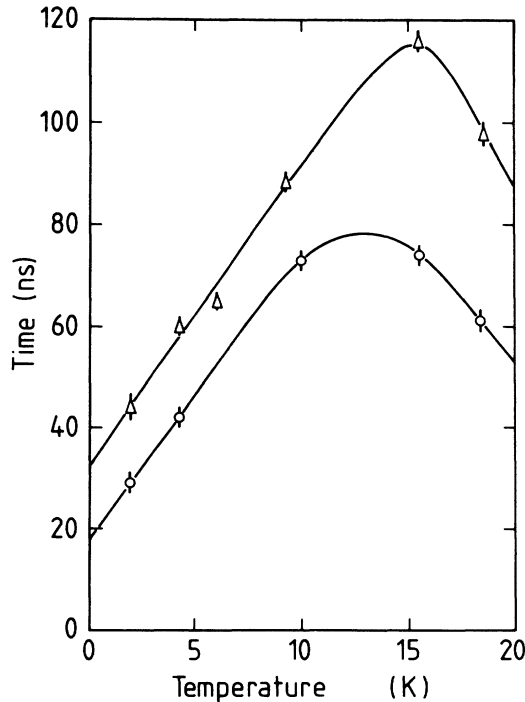

FIG. 3. Temperature dependence of decay time for sample 2 under low-bias conditions. The laser wavelength is 148.5 μm. $\triangle$, resonant $1s$-$2p_+$ PC. $\bigcirc$, cyclotron resonance PC.

prevent dc heating. It is seen that both curves exhibit characteristic maxima at approximately 15 K.

Previous measurements of the PC decay time as a function of temperature have all been made in zero magnetic field. The recombination lifetime for holes at a (deep) copper impurity and at a shallow impurity in p-type Ge have been measured as a function of temperature using a pulsed 10-μm-wavelength laser.[10] Temperature (T) dependencies of the recombination lifetimes of $T^{1.1}$ and $T^{1.8}$ respectively can be deduced for these systems. Recombination lifetimes have also been obtained for the shallow donor in n-type Ge,[35] and a $T^{+2.0}$ behavior noted. We have recently[36] measured the zero-magnetic-field PC decay time for the present samples of InP up to 5 K and have found a simple $T^{+1.7}$ dependence of decay time upon temperature, which is consistent with the foregoing investigations for germanium and which illustrates the universal hydrogenlike character of the phenomenon.

We attribute the characteristic maximum in Fig. 3 to the temperature dependence of both the recombination cross section and the number of recombination centers, i.e., ionized donors.

It is shown elsewhere[21,22] that τ_{eff} is given by an expression of the type

$$\tau_{\text{eff}} = (N_d^+ B_T)^{-1} \ , \qquad (5.1)$$

where N_d^+ is the ionized donor concentration and B_T is the phonon-assisted recombination coefficient. The thermal exhaustion of the neutral donors follows from elementary theory as

$$N_d^+ \approx N_a^- + (N_d - N_a) / [\exp(E_R / kT) + 1] \ , \qquad (5.2)$$

where E_R is the shallow donor ionization energy. B_T will decrease as the temperature is increased due to the thermal reexcitation of electrons in excited bound states.[14]

It seems permissible to assume that at the relatively low magnetic fields used here, the temperature variation of B_T is similar to the zero-field case, i.e.,

$$B_T = B_0 - A_0 T^\alpha \ , \qquad (5.3)$$

with $\alpha \approx 2$. Convolution of (5.2) and (5.3) generates a temperature dependence of τ_{eff} with one characteristic maximum. Taking the experimentally observed zero-field values, together with appropriate sample parameters, it is estimated that this maximum occurs at a value of 15 K, which is in fair agreement with experiment.

B. Magnetic field variation of τ_{eff}

The values of τ_{eff} as measured in these experiments are likely to be controlled by different rate determining steps for samples of differing ionized donor concentrations. Furthermore, it is evident from Figs. 2(a) and 2(b) that any observed differences in τ_{eff} in the CR and $1s$-$2p_+$ cases (at the same magnetic field) will reflect differences in the $2p_+$ and $N = 1$ LL lifetimes.

For the sample with the lowest compensation ratio (sample number 2) it is evident from Fig. 4 that there is little difference between the two values of τ_{eff}, and that
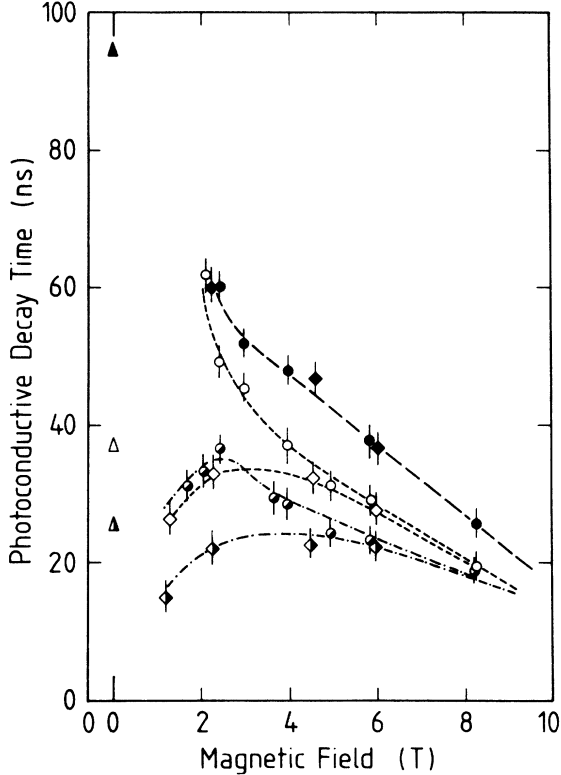
FIG. 4. Decay time as a function of magnetic field for three samples at 4.2 K under resonant $1s$-$2p_+$ and cyclotron resonance (CR) conditions. ○, sample 1, CR; ◇; sample 1, $1s$-$2p_+$. ●: sample 2, CR; ◆: sample 2, $1s$-$2p_+$. ◐ : sample 3, CR; ◈: sample 3, $1s$-$2p_+$.

there is a monotonic decrease in their common value with magnetic field. Allan *et al.*[8] have also noted a decrease in τ_{eff} with magnetic field for an uncompensated sample of GaAs. At zero magnetic field, the value of τ_{eff} for all samples in Fig. 4 is determined by N_a,[36] and at high magnetic fields it approaches a value weakly dependent on N_a, as will be discussed later. The low concentration of ionized donors in sample 2 at 4.2 K, consequent upon the low value of N_a ($\approx 2 \times 10^{-13}$ cm^{-3}), will ensure that the rate determining steps for τ_{eff} are the transitions into the lower-energy bound states such as $2p_-$, $2p_0$, $2s$, etc. Although transitions into a number of such states are possible, considerations of the form of the expression for the transition rate suggest that there will be an optimum final state, typically 0.5–1 meV below the $N=0$ LL. This rate will of course depend on the ionized donor concentration, which under low-excitation conditions will approach N_a. In the previous section it has been shown that τ_{eff} calculated on this basis smoothly decreases with magnetic field, as seen in Fig. 4 for sample 2.

The smooth decrease in τ_{eff} which is experimentally observed for sample 2 is adequately accounted for by the variation in a magnetic field of the phonon-assisted transition rate between a free and a bound state. This discussion is appropriate to the case when $l_B \ll d$ which holds for sample 2. For the other specimens (numbers 1 and 3) it is evident that there is an initial rise in τ_{eff} with field,

after which the measured decay time falls to a high field value which is common to both processes and only weakly dependent on N_a. We now discuss the shorter decay times noted for these more compensated samples at lower magnetic fields. As already mentioned the transition from the $2p_+$ state to the $N=0$ state deposits electrons in a range of angular momentum states, typically from $m=0$ to $m=-4$ for a representative magnetic length, $l_B = 10^{-8}$ m. The spatial extent of a given wave function is of order[37] $2l_B(1-2m)^{1/2} \simeq 10 l_B = 100$ nm for these states, taking $-m=4$. This is comparable with the impurity spacing in the samples with the highest concentration of acceptors. At low fields both M and l_B will be larger and an electron has a choice of going into the bound states of several impurities. Thus the transition rates are larger in the two samples with a greater number of available ionized impurities, and the decay times are therefore shorter as observed. Furthermore, τ_{eff} will increase with magnetic field as the number of available impurity states reduces. However, for higher fields, the electrons are likely only to return to the same impurity: the situation then reverts to the effect discussed above for which τ_{eff} begins to all with field. The characteristic maximum in the graph of τ_{eff} versus B (Fig. 4) for the samples 1 and 3 is therefore explained.

It is assumed in the above argument that the rate of entry of electrons into the $N=0$ LL from the $2p_+$ is fast in comparison with the "electron removal processes" from this level. These processes are again regarded as the rate-determining steps in the value of τ_{eff}. Theoretical justification for this assumption, which is completely contradictory to the experimental inferences of Allan *et al.*[8] for saturation-absorption measurements, is given by the calculations of the previous section. It is also consistent with the interpretation of the data for the least compensated sample discussed above.

As stated earlier, the difference between the measured values of τ_{eff} for CR and $1s$-$2p_+$ cases is to be interpreted as a difference in the $2p_+$ and $N=1$ LL lifetimes. For sample 2 this difference cannot be resolved due to experimental uncertainty. For samples 1 and 3 this difference changes from approximately 10–20 ns at low fields to less than 1 ns (i.e., the experimental accuracy in the determination of τ_{eff}) at higher field. This is consistent with the interpretation that the processes of Figs. 2(a) and 2(b) following electron injection are the same, since the $2p_+$ state pins to the $N=1$ LL at high fields.[25] Furthermore, it is possible to use this difference to estimate the $N=1$ LL lifetime on the assumption that the $2p_+ - N=0$ transition is sufficiently fast that the $2p_+$ lifetime may be neglected, as mentioned above (and discussed in the last section). The $N=1$ LL lifetime is estimated on this basis to vary from 20 ns at low field to less than 1 ns at high field. This trend is consistent with a deformation-potential coupling mechanism for the $N=1-N=0$ LL electronic transition, since the transition rate will then increase as the magnetic field increases the separation of the LL's.

Finally, we turn to the apparent independence of τ_{eff} on N_a for both CR and $1s$-$2p_+$ processes at high magnetic fields. The heuristic interpretation given to this intrigu-

ing result is that in sufficiently high fields an electron, photoionized by the FIR laser, is most likely to return to the same impurity from which it was originally excited. The electron will not sense the presence of other ionized donors and hence the conduction band effective lifetime is independent of N_a as observed. The physical justification for this "magnetic localization" mechanism is that the center of the cyclotron orbit (radius ≈ 10 nm) will drift at a velocity E/B (≈ 5 ms^{-1} under present circumstances). With an effective lifetime of approximately 20 ns at high fields, this gives a drift distance of 100 nm, which is somewhat smaller than the average ionized donor separation. The electron is therefore likely to recombine with the donor impurity to which it was originally bound. This simple picture is also confirmed by the observed drop in PC amplitude as the magnetic field is increased, which is consistent with a drop in net charge transport through the sample. It is noteworthy that at zero magnetic field the drift velocity ($\mu E \approx 100$ ms^{-1}) combined with a lifetime of ~ 50 ns, yields a drift length of ~ 5 μm. This length is larger than either the elastic mean free path or the interimpurity spacing and implies recombination to one of a large number of possible ionized donors.

VI. CONCLUSION

We have shown that the recombination lifetime of photoionized shallow donors in n-type InP depends on both magnetic field and acceptor concentration. These dependencies can be qualitatively understood on the basis of a simple analytic calculation of the transition rates which determine this lifetime. The calculations also show that the differences in lifetime under resonant $1s$-$2p_+$ excitation and cyclotron resonance can be ascribed to the $N=1$ LL lifetime.

ACKNOWLEDGMENTS

APPENDIX

As explained in Sec. IV, we require matrix elements of the deformation potential $\hat{H}_q$ coupling electrons to phonons of wave vector q in order to calculate electronic transition rates for a transition from a bound state to a continuum state due to acoustic phonon emission or absorption. $\hat{H}_q$ is given by

$$\hat{H}_q = -Ci \left[\frac{\hbar}{2MN\omega_q} \right]^{1/2} \mathbf{e}_q \cdot \mathbf{q} \exp(i\mathbf{q}\cdot\mathbf{r}) , \qquad \text{(A1)}$$

where C is the deformation potential coupling constant, $\mathbf{r}$ is the position of an electron, M is the mass of an atom, N is the number of atoms, ω_q and $\mathbf{e}_q$ are, respectively, the frequency and unit polarization vector of phonons of wave vector $\mathbf{q}$ and we use a Debye model for the phonons.

For the states of an electron bound to an impurity in a magnetic field $\mathbf{B}$ along the z axis, we use variational wave functions of the type proposed originally by Yafet et al.[30] and given in a more generalized form by Wallis and Bowlden.[31] We write the wave function for the bound state $\lambda = (l,m,s)$ in cylindrical coordinates as

$$\psi_\lambda(\rho,z,\phi) = n_\lambda \left[\frac{\rho^2}{2a_\lambda^2} \right]^{|m|/2} L_{lm}(\rho^2) P_s(z)$$

$$\times \exp\left[-\frac{\rho^2}{4a_\lambda^2} - \frac{z^2}{4b_\lambda^2} + im\phi \right] , \qquad \text{(A2)}$$

where n_λ is the normalization constant, a_λ and b_λ are the variational parameters for each state and the polynomials $L_{lm}(\rho^2)$ and $P_s(z)$ are chosen so that the wave functions are orthogonal. A representative list of the bound states has been given by Narita and Miyao.[32]

For the continuum states, we use the eigenfunctions of a free electron in a magnetic field. The magnetic potential

$$\mathbf{A} = (-B_y/2, B_x/2, 0)$$

in the symmetric gauge for a magnetic field of strength B along the z axis. The energy levels are

$$E_\lambda = \frac{\hbar\omega_c}{2}(2l + |m| + m + 1) + \frac{\hbar^2 k_z^2}{2m^*} , \qquad \text{(A3)}$$

and the eigenfunctions are (see, for example, Refs. 31 and 37)

$$\psi_\lambda = n_\lambda \left[\frac{\rho^2}{2l_B^2} \right]^{|m|/2} L_{l+|m|}^{|m|} \frac{\rho^2}{2l_B^2}$$

$$\times \exp\left[-\frac{\rho^2}{4l_B^2} + ik_z z + im\phi \right] \qquad \text{(A4)}$$

with

$$n_\lambda^2 = \frac{1}{2\pi l_B^2 L_z} \frac{l!}{[(l+|m|)!]^3} ,$$

where $\lambda = (l,m,k_z)$, n_λ is the normalization constant of the eigenstate, the cyclotron frequency $\omega_c = eB/m^*$, the magnetic length $l_B = (\hbar/eB)^{1/2}$, m^* is the effective mass of an electron, and $L_m^n(x)$ is an associated Laguerre polynomial. It can be seen that all states with $m = -|m|$ are degenerate and the electronic charge distribution is limited to a cylindrical region about the origin whose root-mean-square radius is $2^{1/2}l_B(1+2l+|m|)^{1/2}$. The lowest-lying Landau level is the set of states $(0,-|m|,k_z)$ and it is referred to as the $N=0$ state.

The matrix element $\langle \lambda | \hat{H}_q | \lambda' \rangle$ between a bound state and the $N=0$ state will only be significant when there is appreciable overlap between the two wave func-

tions. It is convenient to take the origin for the magnetic vector potential at the impurity center so that only those states with small $|m|$ give significant matrix elements for the range of magnetic fields of interest.

We illustrate the evaluation of the matrix elements

with those for the $2p_{\pm}$ states. The results are more transparent than the general one and all the other matrix elements can be calculated in a similar fashion. Since $\hat{H}_{-q}$ only depends on an electron position through the factor $\exp(-i\mathbf{q}\cdot\mathbf{r})$, we consider

$$M_{\lambda\lambda'}=\langle\lambda\,|\exp(-i\mathbf{q}\cdot\mathbf{r})\,|\,\lambda'\rangle$$

$$=n_\lambda n_{\lambda'}\int\int\int\rho\exp\left[-\frac{\rho^2}{4a_\lambda^2}-\frac{z^2}{4b_\lambda^2}\mp i\phi\right]\exp(-i\mathbf{q}\cdot\mathbf{r})\left[\frac{\rho^2}{2l_B^2}\right]^{|m|/2}\exp\left[-\frac{\rho^2}{4l_B^2}+ik_z z-i\,|m|\,\phi\right]\rho\,d\rho\,dz\,d\phi\,,$$

$$(A5)$$

where $\lambda=2p_\pm$ and $\lambda'=(0,-\,|m|\,,k_z)$. The z integration is straightforward and gives

$$M_{\lambda\lambda'}=2\pi^{1/2}b_\lambda\exp[-b_\lambda^2(q_z-k_z)^2]$$

$$\times\int\int\exp\left[-\frac{\rho^2}{4}\left[\frac{1}{a_\lambda^2}+\frac{1}{l_B^2}\right]\right]\rho^2\left[\frac{\rho^2}{2l_B^2}\right]^{|m|/2}$$

$$\times\exp[-i(\,|m|\pm1)\phi$$

$$-i\rho(q_x\cos\phi+q_y\sin\phi)]d\rho\,d\phi\,.$$

$$(A6)$$

The ϕ integration gives rise to a Bessel function $J_{m\pm1}(\rho q_\perp)$, where $q_\perp=(q_x^2+q_y^2)^{1/2}$, so that the ρ integration is a Hankel transform. The Hankel transforms can be evaluated for any bound state by using the standard integral

$$\int_0^\infty t^{m+1}\exp(-\alpha^2 t^2)J_m(bt)dt=\frac{b^m}{(2\alpha^2)^{m+1}}\exp\left[-\frac{b^2}{4\alpha^2}\right]$$

$$(A7)$$

and a similar expression for different powers of t which can be determined by using confluent hypergeometric functions.

For $\lambda=2p_+$,

$$|M_{\lambda\lambda'}|=f(\lambda,\lambda')$$

$$=2^{|m|/2+q/4}\pi^{1/4}\left[\frac{a_\lambda^2}{a_\lambda^2+l_B^2}\right]^{|m|+2}$$

$$\times\frac{l_B b_\lambda^{1/2}}{a_\lambda^2 L_z^{1/2}}\frac{(l_B q_\perp)^{|m|+1}}{(\,|m|\,!)^{1/2}}$$

$$\times\exp[-b_\lambda^2(q_z-k_z)^2-c_\lambda a_\lambda l_B q_\perp^2]\,,\qquad(A8)$$

where $c_\lambda=a_\lambda l_B/(a_\lambda{}^2+l_B{}^2)$ and L_z is the length of the sample in the z direction.

For $\lambda=2p_-$,

$$|M_{\lambda\lambda'}|=f(\lambda,\lambda')\left|\frac{|m|}{c_\lambda a_\lambda l_B q_\perp^2}-1\right|\,.\qquad(A9)$$

The matrix elements for all bound states involve the same factor $f(\lambda,\lambda')$ and it largely determines the dependence of the decay times on magnetic field.

We consider next the transitions from the $N=0$ state into a lower bound state and from the $2p_+$ state into the $N=0$ state. The former occurs only by phonon emission. The latter, however, is by phonon absorption when the $N=0$ state is at higher energy at low B, and by both emission and absorption at higher fields when the two states switch over. We outline here the calculation of the transition rates due to phonon emission. Those due to phonon absorption are evaluated in a similar way.

We determine first the transition rate Γ_C for transitions from the $\lambda=2p_+$ state into the $N=0$ state due to all possible emitted phonons. It is given by

$$\Gamma_C=\frac{C^2 L_z}{8\pi^2\rho v_s}\sum_{m=0}^{S}\int\int\int q^3\,|M_{\lambda\lambda'}|^2\,\delta(E_\lambda-E_{\lambda'}-\hbar\omega_q)\sin\theta\,d\theta\,dq\,dk_z$$

$$=\left[\frac{2}{\pi}\right]^{3/2}\frac{C^2 b_\lambda}{\hbar\rho v_s^2}c_\lambda^4\int_{-k_m}^{k_m}dk_z\int_0^\pi d\theta\sin\theta(l_B q\sin\theta)^2 q^3\exp[2b_\lambda^2(q\cos\theta-k_z)^2-2c_\lambda a_\lambda l_B(q\sin\theta)^2]$$

$$\times\sum_{m=0}^{S}\frac{1}{m!}(2^{1/2}c_\lambda a_\lambda q\sin\theta)^{2m}\,,\qquad(A10)$$

where

$$q = q(k_z) = \left| E_\lambda - \frac{\hbar\omega_c}{2} \frac{h^2 k_z^2}{2m^*} \right| \bigg/ \hbar v_s \; ,$$

$$\hbar k_m = [(2E_\lambda - \hbar\omega_c)m^*]^{1/2} \; .$$

ρ and v_s are, respectively, the density and velocity of sound in InP, θ is the angle between q and the z axis, S is the number of $(0, -|m|, k_z)$ states which are confined within the sample, and, for simplicity, we have omitted the factor n_q for stimulated emission. For all practical purposes, there are no size effects and S can be taken to be infinite. Therefore the m summation produces an exponential factor. The terms of this sum also indicate the size of the transition rate for each value of $-|m|$ and this is used in Sec. IV. The remaining integrals can be manipulated to give

$$\Gamma_C = \frac{2b_\lambda c_\lambda^4 C^2}{\pi d_\lambda h \rho v_s^2} \int_{-k_m}^{k_m} dk_z q^2 (l_B q)^2 \exp[-2c_\lambda^2 l_B^2(q^2 - k_z^2 b_\lambda^2/d_\lambda^2)] \left| (1 - \beta^2/4\alpha^4)\phi_0(\alpha + \beta/2\alpha) - \frac{1}{2\alpha^2}\phi_2(\alpha + \beta/2\alpha) \right| \; ,$$

(A11)

where

$$d_\lambda^2 = b_\lambda^2 - c_\lambda^2 l_B^2, \quad \alpha = 2^{1/2} d_\lambda q, \quad \beta = 4b_\lambda^2 k_z q \; ,$$

and

$$\phi_n(u) = \frac{2n}{\sqrt{\pi}} \int_0^u t^n e^{-t^2} dt \; .$$

We now consider the transition rate Γ_B' for transitions into a bound state due to all possible emitted phonons and summed over all initial m and k_z for the $N=0$ state in order to obtain an average rate as discussed in Sec. IV. We present the result for the $\lambda = 2p_-$ state which reveals the essential features of Γ_B' for any of the relevant bound states. We find that

$$\Gamma_B' = \frac{4b_\lambda c_\lambda^4 C^2}{\pi d_\lambda h \rho v_s^2} \int_{-\infty}^{\infty} dk_z q^2 \exp[-2c_\lambda^2 l_B^2(q^2 - k_z^2 b_\lambda^2/d_\lambda^2)]$$

$$\times \left[\left[1 + \frac{(ql_B e_\lambda)^2}{2} \right] \phi_0(\alpha + \beta/2\alpha) - \frac{1}{2} \left[\phi_2(\alpha + \beta/2\alpha) + \frac{4b_\lambda^4 k_z^2}{d_\lambda^2} \phi_0(\alpha + \beta/2\alpha) \right] \left[\frac{l_B e_\lambda}{2d_\lambda} \right]^2 \right] \; ,$$

where

$$e_\lambda = \frac{l_B^2 - a_\lambda^2}{l_B^2 + a_\lambda^2} \; .$$

(A12)

In evaluating Γ_B' and Γ_C, it is a good approximation to set $\phi_0 = \phi_2 \cong 1$. As discussed in Sec. IV, the $2s$ and low-lying $n=3$ states are more likely to control the loss of electrons from the $N=0$ state. They have Γ_B''s which are formally similar to the above. In particular, the $3p_-$ state differs from the $2p_-$ only by a factor of $(1 - Dz^2)$ in the wave function. Therefore the results are very similar since the z interaction has a relatively minor part to play in the analysis.

*Also at the Research Institute for Materials, University of Nijmegen, Toernooiveld, NL 6525-ED, Nijmegen, The Netherlands.

[1]C. J. Armistead, P. Knowles, S. P. Najda, and R. A. Stradling, J. Phys. C 17, 6415 (1984).

[2]R. F. Kirkman and R. A. Stradling, J. Phys. C 6, L324 (1973).

[3]C. J. Armistead, P. C. Makado, S. P. Najda, and R. A. Stradling, J. Phys. C 19, 6023 (1986).

[4]C. J. Armistead, S. P. Najda, R. A. Stradling, and J. C. Maan, Solid State Commun. 53, 1109 (1985).

[5]A. A. Reeder, J. M. Chamberlain, R. J. Turner, and G. Hill, Solid State Commun. 57, 355 (1986).

[6]T. S. Low, G. E. Stillman, A. Y. Cho, H. Morkoç, and A. R. Calawa, Appl. Phys. Lett. 40, 611 (1982).

[7]P. C. Makado and N. C. McGill, J. Phys. C 19, 873 (1986).

[8]G. R. Allan, A. Black, C. R. Pidgeon, E. Gornik, W. Seidenbusck, and P. Colter, Phys. Rev. B 31, 3560 (1985).

[9]M. Asche, H. Kostial, and O. G. Sarbey, Phys. Status. Solidi B 91, 521 (1979).

[10]P. Norton and H. Levinstein, Phys. Rev. B 6, 489 (1972).

[11]Sh. M. Kogan, Fiz. Tverd. Tela (Leningrad) 4, 1813 (1963) [Sov. Phys.—Solid State 4, 1813 (1963)].

[12]G. Ascarelli and S. Rodriguez, Phys. Rev. 124, 1321 (1961).

[13]J. M. Chamberlain, A. A. Reeder, L. M. Claessen, G. L. J. A. Rikken, and P. Wyder, Phys. Rev. B 35, 2391 (1987).

[14]R. A. Brown and S. Rodriguez, Phys. Rev. 153, 890 (1967).

[15]C. R. Pidgeon, A. Vass, G. R. Allan, W. Prettl, and L. Eaves, Phys. Rev. Lett. 50, 1309 (1983).

[16]H. J. A. Bluyssen, J. C. Maan, T. B. Tan, and P. Wyder, Phys. Rev. B 22, 749 (1980); H. J. A. Bluyssen, J. C. Maan, and P. Wyder, Solid State Commun. 31, 465 (1979).

[17]See, for example, E. Gornik, in Lecture Notes in Physics, edited by W. Zawadski (Springer, Berlin, 1980), Vol. 133, p. 160.

[18]W. Muller, E. Gornik, T. J. Bridges, and T. Y. Chang, Solid State Electron. 21, 1455 (1978).

[19]L. L. Taylor and D. Anderson, J. Cryst. Growth 64, 55 (1983).

[20]H. Salzmann, T. Vogel, and G. Dodel, Opt. Commun. 47, 340 (1983).

[21]G. L. J. A. Rikken, P. Wyder, J. M. Chamberlain, and L. L. Taylor, Europhys. Lett. 5, 61 (1988).

[22]G. L. J. A. Rikken, P. Wyder, J. M. Chamberlain, R. T. Grimes, and L. L. Taylor, Phys. Rev. B (to be published).

[23]H. C. Praddaude; Phys. Rev. A 6, 1321 (1972).

[24]J. B. McManus, R. People, R. L. Aggarwal, and P. A. Wolff, J. Appl. Phys. 52, 4748 (1981).

[25]W. S. Boyle and R. E. Howard, J. Phys. Chem. Solids 19, 181 (1961).

[26]F. Beleznay and G. Pataki, Phys. Status Solidi 13, 499 (1966).

[27]H. Forster, W. Strupat, W. Rosner, G. Wunner, H. Ruder, and H. Herold, J. Phys. B 17, 1301 (1984).

[28]W. Rosner, G. Wunner, H. Herold, and H. Ruder, J. Phys. B 17, 29 (1984).

[29]H. Ruder, G. Wunner, H. Herold, and M. Reinecke, J. Phys. B 14, L45 (1981).

[30]Y. Yafet, R. W. Keyes, and E. N. Adams, J. Phys. Chem. Solids 1, 137 (1956).

[31]R. F. Wallis and H. J. Bowlden, J. Phys. Chem. Solids 7, 78 (1958).

[32]S. Narita and M. Miyao, Solid-State Commun. 9, 2161 (1971).

[33]W. Kohn and J. M. Luttinger, Phys. Rev. 98, 915 (1955).

[34]D. M. Larsen, J. Phys. Chem. Solids 29, 271 (1968).

[35]S. H. Koenig, R. D. Brown, and W. Schillinger, Phys. Rev. 128, 1668 (1962).

[36]G. L. J. A. Rikken, P. Wyder, J. M. Chamberlain, D. P. Halliday, and R. T. Grimes, Solid State Electron. 81, 763 (1988).

[37]R. H. Garstang, Rep. Prog. Phys. 40, 105 (1977).